MJFAS
Malaysian Journal of Fundamental and Applied Sciences

Suhaimi *et al.* | Malaysian Journal of Fundamental and Applied Sciences, Vol. 21 (2025) 1907-1927

RESEARCH ARTICLE

Synthesis and Characterization of Honey-Pectin Hydrogel: Exploring Potential Applications in Wound Healing

Hazwani Suhaimi[a]*, Nabihah Murdini[a], Norazanita Shamsuddin[a], Azman Ma'amor[b], Pg Emeroylariffion Abas [a]

[a]Faculty of Integrated Technologies, Universiti Brunei Darussalam, Jalan Tungku Link, Gadong BE1410, Brunei; [b]Chemistry Department, Faculty of Science, Universiti Malaya, 50603 Kuala Lumpur, Malaysia

Abstract Hydrogels have garnered considerable interest as dynamic platforms for wound healing due to their ability to maintain a moist environment and promote tissue regeneration. This study explores the synthesis and characterization of honey-pectin hydrogels, leveraging the natural healing properties of honey combined with the biocompatibility of pectin. Employing a solution casting method, hydrogels with varied honey concentrations were prepared and examined to ascertain their suitability for wound care applications. The hydrogels were subjected to a series of characterization techniques including Scanning Electron Microscopy (SEM), Fourier Transform Infrared Spectroscopy (FTIR), Swelling Tests, and Hydrogel Dehydration Rate Testing (HDRT) analyses. The SEM and FTIR results demonstrated that the inclusion of honey not only enhanced the structural integrity but also enriched the chemical stability of the hydrogels. Swelling tests revealed that the hydrogels could effectively absorb and retain moisture, a crucial function for preventing wound desiccation. Additionally, the HDRT results demonstrated that the hydrogels adequately managed moisture release, a critical factor in preventing maceration while supporting natural healing processes; with the dehydration rate ranged from 37.24 to 50.02 g/m^2/h and 11.03 to 31.58 g/m^2/h, for the air-dried and the vacuum-dried hydrogels, respectively. This study highlights the potential of honey-pectin hydrogels as effective wound dressings that can be tailored to meet specific clinical requirements and sets the stage for further development and clinical testing to enhance their therapeutic efficacy and usability in medical applications.

Keywords: Hydrogel, wound healing, honey, pectin, moisture management.

Introduction

***For correspondence:**
hazwani.suhaimi@ubd.edu.bn

Received: 01 Oct. 2024
Accepted: 05 March 2025

The skin serves as a crucial barrier, protecting the body from external threats such as pathogens, chemicals, and physical trauma. When this protective barrier is compromised by thermal or physical trauma, it results in a wound [1], triggering a complex healing process influenced by a myriad of internal and external factors. Internally, factors such as impaired local blood supply can slow down the healing process by restricting nutrient and oxygen delivery to the wound site. External factors such as surgical interventions, trauma, heat, electrical currents, chemical exposure, and extreme temperatures can cause tissue damage and initiate the wound healing cascade [2,3].

Traditionally, the initial stages of wound care have relied on dry dressings such as gauze and cotton wool. These materials, however, often fail to maintain an optimal moist environment for proper wound healing, leading to issues like dehydration and wound trauma upon removal. Additionally, these conventional dressings lack properties such as antimicrobial and antioxidant activities, crucial for preventing infection and promoting healing [4]. An ideal wound dressing should overcome these shortcomings by effectively maintaining a moist environment conducive to proper cell adhesion and proliferation while preventing bacterial contamination [5]. It should also have the ability to absorb excess exudate produced during the healing process, as excessive or insufficient exudate can hinder healing

progress [6,7]. Furthermore, the dressing should be non-toxic, possess appropriate viscosity and mechanical characteristics, facilitate the gas exchange to promote oxygenation of the wound bed, and absorb tissue fluid efficiently to maintain a clean and healthy wound environment. Recent advancements in wound dressing technology have seen the development of hydrogels that incorporate bioactive substances like honey and pectin, aim to fulfil these criteria and provide an optimal environment for wound healing. By addressing the multifaceted needs of wound care, these advanced dressings offer promising solutions to enhance the healing process and improve patient outcomes.

Hydrogels offer several advantages in wound healing due to their unique properties. Their ability to retain a large amount of water or biological fluids makes them effective in crucially maintaining a moist environment conducive to effective healing [8]. This moisture-rich setting not only reduces the risk of infection but also facilitates autolytic debridement, a natural breakdown of dead tissue [9,10]. One notable feature of hydrogel-based dressings is their porous structure, which allows for the targeted release of substances, including drugs or bioactive molecules, at specific locations within the wound [1]. This controlled release can enhance the therapeutic effect and aid in the healing process. Moreover, hydrogels can help regulate the microclimate over the wound, allowing nutrients and oxygen to reach the wound bed, which is vital for tissue regeneration and cell proliferation [11]. Their cooling effect can also help reduce inflammation and alleviate pain, contributing to patient comfort during the healing process [12]. By absorbing excess exudate, hydrogels help maintain the ideal moisture balance, preventing maceration and promoting the formation of granulation tissue. Overall, the unique qualities of hydrogels make them promising candidates in the field of wound care, offering a supportive environment for tissue repair and regeneration [1].

The use of both natural and synthetic polymers, or a combination thereof, in hydrogel formulations offers a wide range of options for tailoring hydrogel properties to specific wound healing needs. Natural polymers such as collagen, hyaluronic acid, chitosan, alginate, and particularly, pectin have gained attention due to their biocompatibility and ability to be modified to produce hydrogels with desired characteristics [13]. Pectin, derived from plant cell walls, is a natural polymer with biocompatible and biodegradable properties, making it suitable for biomedical applications [14-18]. Pectin hydrogels can create a moist environment necessary for tissue regeneration and wound healing, while also absorbing and retaining water to maintain proper moisture balance in wound dressings. Additionally, their pH-responsive nature allows for the controlled release of medications or bioactive substances in response to physiological conditions. This makes them attractive for drug delivery systems [19]. With their ability to enhance cell adhesion and proliferation due to high galacturonic acid content, pectin hydrogels hold promise for tissue engineering applications as well. Overall, the diverse properties of natural polymers make them valuable components in hydrogel formulations for wound healing and other biomedical applications.

On the other hand, honey has been utilized since ancient times for its therapeutic properties in wound healing, with numerous studies demonstrating the antibacterial, antiviral, anti-inflammatory, and antioxidant properties of honey, making it suitable for treating various types of wounds [20,21]. The antibacterial properties of honey are attributed to the production of hydrogen peroxide production via glucose oxidase activity as well as its high osmolarity and acidity [22-25]. Incorporating honey into hydrogel matrices, such as those based on chitosan, has been shown to enhance wound healing outcomes [26]. The controlled release of honey from the hydrogel dressing can promote the formation of new blood vessels and the regeneration of epidermal tissue, facilitating the healing process [26]. The synergistic integration of honey and pectin as medical hydrogels for wound treatment has indeed shown considerable potential to accelerate the wound healing process, as reported by Giusto *et al*. [27,28] and Cerullo *et al*. [29], highlighting their efficacy in enhancing tissue regeneration and offering antimicrobial protection. While previous similar studies have investigated honey-based hydrogels, the application of raw, locally sourced stingless bee honey in functional wound dressings remains unexplored. Most research has focused on commercial honey varieties, leaving a gap in understanding the benefits of locally sourced, raw stingless bee honey. This body of work provides a critical foundation for our study, wherein we explore nuanced variations in honey and pectin ratios and their implications for hydrogel performance.

Indeed, maintaining a moist environment around the wound is crucial for optimal healing. Dressings that can achieve this while also providing antimicrobial properties and absorbing excess exudate are highly beneficial. Advances in wound care technology have led to the development of various types of dressings, such as hydrogels, foams, films, and hydrocolloids, each with its own unique properties suited for different types of wounds and stages of healing. Integrating bioactive substances into dressings further enhances their therapeutic potential, promoting faster healing and reducing the risk of infection. By preparing honey-based hydrogels with varying amounts of locally sourced honey and using pectin as a crosslinker, this paper aims to investigate the influence of honey concentration on the properties of the hydrogels,

particularly in terms of swelling behavior, Hydrogel Dehydration Rate Testing (HDRT), and structural characteristics. Overall, the combination of these characterization techniques provides a comprehensive understanding of the honey-based hydrogels' properties and their potential applications in wound healing and other biomedical fields. By systematically adjusting the formulation, we seek to maximize its healing efficiency while maintaining a sustainable and cost-effective approach. This research not only introduces a novel combination of materials but also addresses the potential of regionally available natural resources in wound healing applications.

Materials and Methods

This section outlines the comprehensive methodologies employed in the synthesis and characterization of honey-pectin hydrogels designed for wound healing applications. It details the precise steps taken to prepare the hydrogel samples with varying concentrations of honey and pectin, ensuring consistency and reproducibility in the formulations. Subsequently, the section describes a series of characterization techniques—Scanning Electron Microscopy (SEM), Fourier Transform Infrared Spectroscopy (FTIR), Swelling Test Analysis, and Hydrogel Dehydration Rate Testing (HDRT) Analysis—each chosen to evaluate distinct properties of the hydrogels crucial for their intended medical use. These methods collectively provide insights into the structural integrity, chemical composition, hydration ability, and moisture management capabilities of the hydrogels, forming the basis for assessing their efficacy in facilitating optimal wound healing conditions.

Preparation of Honey-Pectin Hydrogel

The synthesis of the honey-pectin hydrogels was methodically conducted using locally sourced raw stingless bee honey, particularly, from the Heterotrigona itama stingless bee species, and commercially available pectin powder, from citrus peel. To systematically investigate the influence of varying honey concentrations on the hydrogel properties, five different hydrogel formulations were prepared, as detailed in Table 1. These formulations were differentiated primarily by the volume of honey used, maintaining a consistent quantity of 18g of pectin across all samples. The preparation process was designed to ensure a total water content of 60ml in each hydrogel mixture, accounting for the inherent water content of the honey used. This was achieved by adjusting the volume of deionized water added based on the water already present in the honey, ensuring that each formulation reached the desired water balance. This careful adjustment was critical for maintaining consistency in the hydrogel's physical properties across different samples. The preparation of the honey-pectin hydrogel is composed of five main steps, as depicted in Figure 1.

Table 1. Honey-pectin samples utilised in the preparations of the hydrogel samples

Sample number	Volume of honey (ml)	Volume of water already present in the honey (ml)	Volume of deionized water added (ml)	Mass of pectin added (g)
1 (control)	0	0	60	18
2	20	6.22	53.78	18
3	40	12.44	47.56	18
4	60	18.66	41.34	18
5	80	24.88	35.12	18

Figure 1. Steps of the experimental methodology

1. Initial Water Content Measurement: The preparation process commenced with the measurement of the water content in the honey using a digital refractometer (YIERYI DR301). This step was critical to ensure that the total water content of each hydrogel formulation was accurately maintained at 60 ml, which is crucial for achieving the desired consistency and performance of the hydrogels.
2. Solution Preparation: The honey and deionized water were combined in specified ratios to standardize the total water content across all samples. For instance, in one of the preparations, 20 ml of honey naturally containing 6.22 ml of water and 53.78 ml of deionized water were mixed in a beaker. This mixture was heated to 100°C and stirred continuously to ensure complete dissolution of the honey, forming a homogeneous solution.

3. Pectin Incorporation: After achieving a uniform honey solution, 18 g of pectin powder was gradually incorporated. The mixture was stirred continuously to prevent any lumps and ensure a smooth consistency. This pectin-enriched solution forms the gel matrix, which is foundational to the hydrogel's structure.
4. Casting and Drying: The final solution was then cast onto a tray to a predefined thickness of 2 mm and dried in an oven (Tefal) at 40°C for six hours. Post oven-drying, the hydrogel film was segmented into 5x5 cm pieces. These segments were subjected to further stabilization through air drying at room temperature for five days and an additional 30 minutes of vacuum drying.
5. Sample Variability and Repetition: This methodology was consistently applied to create a series of hydrogel samples with varying volumes of honey (0 ml, 20 ml, 40 ml, 60 ml, and 80 ml). The volume of deionized water was adjusted in each preparation to maintain a total water content at 60 ml, thus ensuring uniform hydrogel properties. These variations in honey content were intended to explore its impact on the hydrogel's physical and chemical characteristics, as detailed in Table 1. Each of these samples is in the form of hydrogel film with a consistent thickness of 2 mm. Sample number 1, with no honey present, is considered the control sample in this study.

Characterization and Analysis

Following the meticulous synthesis of the five honey-pectin hydrogel samples, comprehensive characterization and analysis were performed to evaluate their structural and functional properties. These analyses are pivotal in determining the efficacy of the hydrogels for wound healing applications, focusing on their microstructural composition, chemical functionality, hydration capabilities, and moisture management properties. The characterization process utilizes a series of sophisticated techniques, each aimed at uncovering specific aspects of the hydrogels that are critical for their performance in a clinical setting.

Scanning Electron Microscopy (SEM) Characterization

Scanning Electron Microscopy (SEM) (JEOL JSM-7600F) plays a pivotal role in the characterization of hydrogel dressings by providing high-resolution images of their surface morphology. This technique is essential for assessing the microstructural properties of the honey-pectin hydrogels, which directly influence their functionality in wound healing applications. For the SEM analysis of hydrogel samples, a platinum coating was applied to enhance conductivity, enabling clear and detailed imaging by preventing charging effects. The SEM was conducted at an electron beam voltage of 0.8 to 1.0 kV, optimized to both protect the samples from damage and reveal the detailed porous structure crucial for evaluating the moisture absorption and retention properties of the hydrogels, which are essential for effective wound dressings.

The SEM images reveal how different honey concentrations influence the hydrogel's microstructure, particularly its network density and pore size, impacting the material's mechanical strength and moisture management. Such insights are critical for customizing hydrogel formulations to meet the specific needs of various wound types, ensuring optimal healing conditions through moisture balance, cell migration, and gas exchange [30,31]. The analysis aims to link these structural properties with the hydrogel's functional performance, guiding further refinements to improve its clinical effectiveness.

Fourier Transform Infrared Spectroscopy (FTIR) Characterization

Fourier Transform Infrared Spectroscopy (FTIR) (SHIMADZU IRAffinity-1) is a critical analytical technique used to characterize the chemical properties of honey-pectin hydrogels. This method provides a deeper understanding of the molecular interactions and the composition of the hydrogels by identifying specific functional groups and chemical bonds. For the FTIR analysis of the hydrogel samples, the sample slot was initially cleaned with acetone. Subsequently, the samples were placed carefully on a diamond-plated sampler. The detector was then inserted into its designated slot to commence the analysis. FTIR analysis was conducted across a comprehensive range of wavenumbers, from 4000 cm^{-1} to 400 cm^{-1}, which encompasses the entire spectrum necessary to detect a wide array of organic functional groups. This broad range allows for the detection of both strong and weak bonds, including hydrogen bonds and covalent bonds, which are fundamental to understanding the structural integrity and stability of the hydrogel.

FTIR spectra identify key functional groups—hydroxyl, carbonyl, and carboxylate—in the hydrogel, indicating successful incorporation of honey and pectin and effective cross-linking. This cross-linking is essential for the hydrogel's mechanical strength, swelling capacity, and its ability to maintain a moist healing environment. Additionally, FTIR analysis confirms the purity and consistency of the hydrogel batches, allowing researchers to ensure uniformity and the absence of contaminants, crucial for clinical safety and effectiveness.

Swelling Test Analysis

Swelling capacity of the hydrogel samples is a critical parameter that directly affects their efficacy in wound healing. The ability to absorb and retain moisture within the hydrogel structure not only ensures a conducive environment for wound repair but also impacts the delivery of therapeutic agents. As such, the swelling test was conducted to evaluate how well the hydrogels could manage moisture, an essential feature for preventing wound desiccation and promoting healing processes.

For this analysis, hydrogel samples subjected to both air drying and vacuum drying were weighed (denoted as W_{dry} for weight of dry sample) and then placed in a beaker containing 2 ml of phosphate-buffered saline (PBS) at pH 7.4, simulating the wound site environment. The beaker was placed on a magnetic stirrer plate to ensure consistent interaction between the hydrogel and the buffer, and the temperature was maintained at 37°C, mimicking the human body's internal temperature. At specific time intervals, samples were carefully removed from the buffer solution. To accurately gauge the amount of fluid absorbed, the hydrogels were sandwiched between two paper towels to remove excess surface water before being weighed again (denoted as W_{wet} for the weight of the swollen sample). This step is crucial to ensure that measurements reflect the actual water absorbed by the hydrogel rather than merely surface moisture. The degree of swelling, D_s, was calculated as:

$$D_s = \frac{W_{wet} - W_{dry}}{W_{dry}} \times 100\% \quad (1)$$

This equation provides a quantitative measure of the hydrogel's swelling capacity, reflecting its ability to absorb physiological fluids. Higher swelling ratios indicate a greater ability to maintain moisture, which is vital for creating a protective barrier over the wound and supporting natural healing mechanisms.

The experiment was repeated three times for each sample to ensure consistency and reliability of the data. Analyzing the swelling behavior under different drying conditions (air-dried versus vacuum-dried) also offers insights into the structural differences and efficacy of the drying methods, impacting the performance of the hydrogel in real-world applications.

Hydrogel Dehydration Rate Test (HDRT) Analysis

Hydrogel Dehydration Rate Testing (HDRT) is a critical evaluation process that focuses on the rate at which a hydrogel loses moisture under simulated physiological conditions. While closely related to the Water Vapor Transmission Rate (WVTR), which assesses the ability of materials to allow moisture vapor to pass through, HDRT specifically measures the dehydration characteristics of hydrogels. This test is vital for applications like wound dressings, where managing moisture balance is crucial to prevent wound desiccation or maceration.

The HDRT test was carried out by placing a hydrogel sample over the mouth of a beaker filled with 5 ml of phosphate-buffer solution to simulate a moist wound environment. Subsequently, the beaker was placed in an incubator (N-BIOTEK MINI-CELL NB203M) set at a constant temperature of 37°C and a relative humidity of 35%, conditions that mimic those of a human body environment near a wound site. To quantify the hydrogel's moisture loss, the weight of the hydrogel was recorded every 10 minutes over a duration of 3 hours i.e. 180 minutes. This frequent measurement schedule is designed to provide a precise understanding of the hydrogel's dehydration dynamics. The results from HDRT provide insights into the hydrogel's intrinsic water retention and release capabilities, reflecting its potential performance as a wound dressing:

$$HDRT\left(\frac{g}{m^{2h}}\right) = \frac{W_i - W_f}{3 \times A} \quad (2)$$

where W_i is the initial weight of the sample, W_f is the final weight after 3 hours, and A represents the surface area of the beaker mouth. This metric quantifies the amount of water the hydrogel can lose per hour per square meter, which indirectly relates to its WVTR. A high HDRT rate indicates a hydrogel that effectively releases excess moisture, aligning with desirable characteristics for WVTR in wound healing contexts.

To ensure the reliability of the results, the HDRT was repeated three times for each sample. This repetition helps in confirming the consistency of the hydrogel's moisture management properties. The outcomes of the HDRT are crucial in evaluating whether the hydrogel can maintain the delicate moisture balance required for optimal wound healing, and they provide foundational data that complements broader WVTR assessments, ensuring the hydrogel's suitability for clinical use in wound care settings.

The results from this analysis were given and discussed in Section 3, where the overall performance of the hydrogels in terms of their swelling properties, moisture management, and structural integrity is discussed, setting the stage for concluding their suitability for clinical use in wound care.

Results and Discussions

The honey-pectin hydrogels were synthesized using locally sourced raw honey from the stingless bee species Heterotrigona itama, and commercially available pectin powder derived from citrus peel. Five distinct formulations were prepared, adjusting the volume of honey while maintaining a consistent mass of 18g of pectin in each sample. Each mixture contained a total water content of 60ml, accounting for the inherent water present in the honey. The volume of deionized water added was adjusted accordingly to achieve the desired water balance for each formulation. This meticulous adjustment was crucial to ensure uniformity in the physical properties of the hydrogels across all samples.

Following these preparations, various characterization techniques were employed to explore the impact of different honey concentrations on the hydrogels' properties. These included Scanning Electron Microscopy (SEM), Fourier Transform Infrared Spectroscopy (FTIR), Swelling Test Analysis, and Hydrogel Dehydration Rate Testing (HDRT) Analysis. The findings from these analyses are discussed in the subsequent sections, providing insights into the hydrogels' behaviour under different analytical conditions.

Scanning Electron Microscopy (SEM)

The Scanning Electron Microscopy (SEM) analysis captured detailed images that demonstrate the structural differences between control samples and honey-pectin hydrogels with varying honey concentrations. Figure 2 presents the morphology of the control sample (with 0% honey), while Figure 3 illustrates the morphology of hydrogels treated with different drying methods and increasing amounts of honey.

Figure 2 reveals noticeable brittle molecular aggregates in the control sample, indicative of less cohesive structural formations of pectin surface. Contrastingly, Figure 3 is organized to highlight the effects of honey concentration on the hydrogel structure across two drying methods. The top row shows air-dried samples, and the bottom row displays vacuum-dried samples, with each row progressively increasing the amount of honey from left to right.

In Figure 3, the hydrogels demonstrate that increasing honey content reduces the presence of molecular aggregates, resulting in tighter and more defined network structures. These improved structures suggest a more stable and cohesive matrix. The interactions primarily involve hydrogen bonding facilitated by the hydroxyl (O-H) groups present in both honey and pectin, contributing to the formation of a denser network within the hydrogels. This may be attributed to the plasticization effect of honey, where its presence in the hydrogel matrix can lead to a more flexible and less aggregated structure. This characteristic is reflected in the smoother surface observed in the fabricated hydrogel. Additionally, honey may interfere with pectin crystallization by interacting with pectin molecules or occupying space within the matrix where crystallization would otherwise occur. Consequently, SEM images show a smoother composite surface due to reduced crystallinity.

Notably, SEM analysis shows that air-dried hydrogels exhibit a more uniform and consistent network structure compared to vacuum-dried hydrogels. This observed uniformity suggests that the air-drying process may help in maintaining a more consistent matrix, which could be indicative of a potentially more robust structure. However, it is important to clarify that these observations do not directly measure mechanical stability. Instead, they suggest that air drying may influence the physical properties of the hydrogels, which could impact their potential efficacy in medical applications. The apparent enhancements in network structure are inferred to result from physical interactions facilitated by the drying process, rather than chemical cross-linking. This interpretation aligns with the observed differences in network density and uniformity, providing insights into how drying techniques could potentially affect the functionality of the hydrogel. Further mechanical testing would be necessary to substantiate any claims regarding the mechanical stability of the hydrogels.

The lack of porosity observed in Figure 3 may be attributed to several factors, including the sample preparation, degree of cross-linking, and the pore size distribution. One of the steps of the experimental methodology involved drying process. Additionally, SEM imaging typically requires the sample to be dry; during this process, the fabricated hydrogels, which are initially composed of high water content, can collapse or lose their original structure. This collapse can lead to a film-like appearance rather than the

porous structure that exists when the hydrogel is fully hydrated. Additionally, hydrogels can have very small pores, which may not be clearly resolved or distinguished in SEM images depending on the resolution capabilities of the microscope. If the pores are smaller than the resolution limit of the SEM, they may appear as a homogeneous film rather than a porous network. This does not necessarily mean, however, that the fabricated hydrogels lack porosity in its native hydrated state but rather underscores the challenges in visualizing and interpreting the internal structure of hydrogels using SEM alone. To confirm the presence of porosity in hydrogels, other techniques such as transmission electron microscopy (TEM), confocal microscopy, or porosity analysis methods can be employed. These techniques can provide complementary information about the internal structure and porosity of hydrogels.

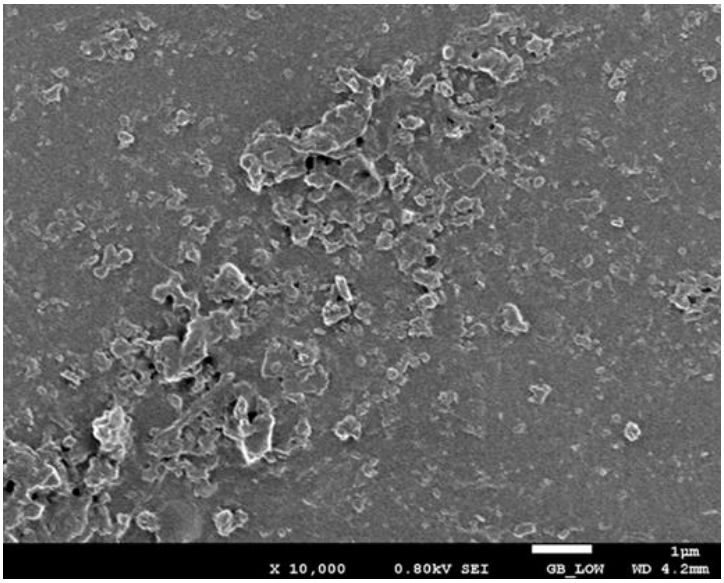

Figure 2. The morphology of the control sample (sample 1: 0% honey)

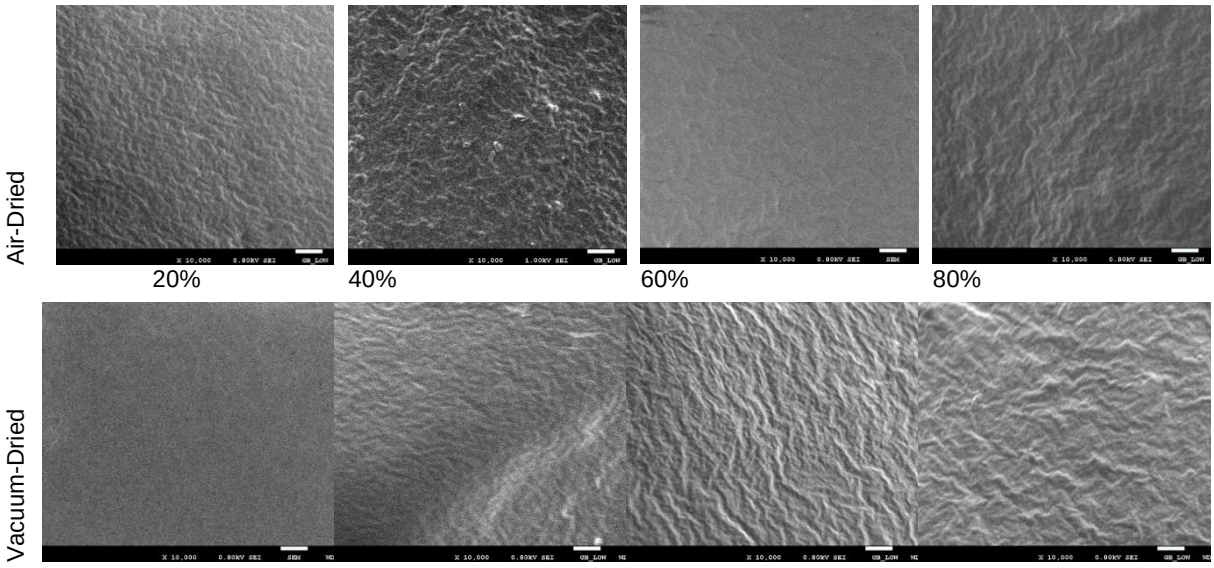

Figure 3. The morphology of air-dried honey-pectin hydrogels (top images) with increasing amounts of honey (from left to right); and vacuum-dried honey-pectin hydrogels (bottom images) with increasing amounts of honey (from left to right)

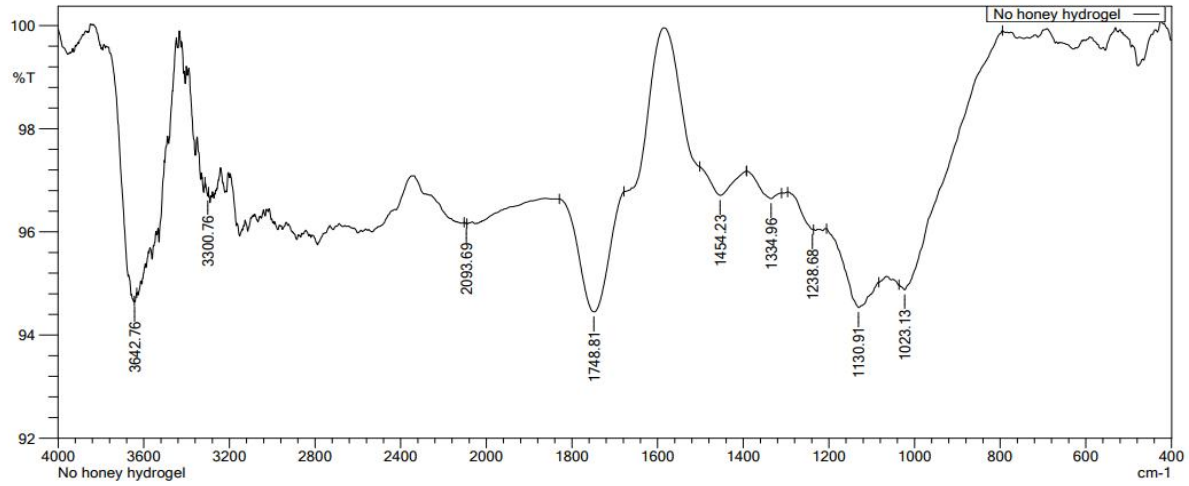

(a)

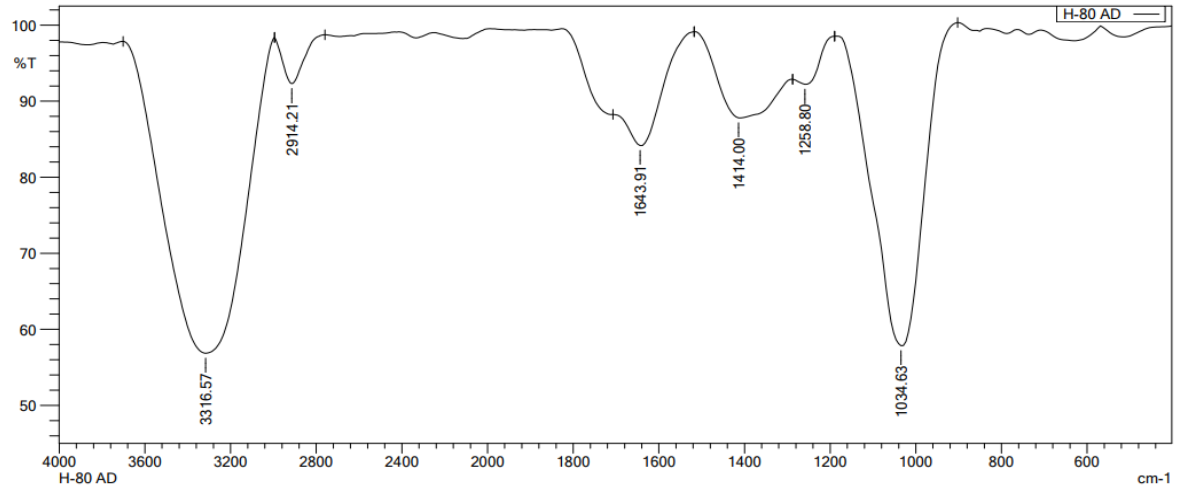

(b)

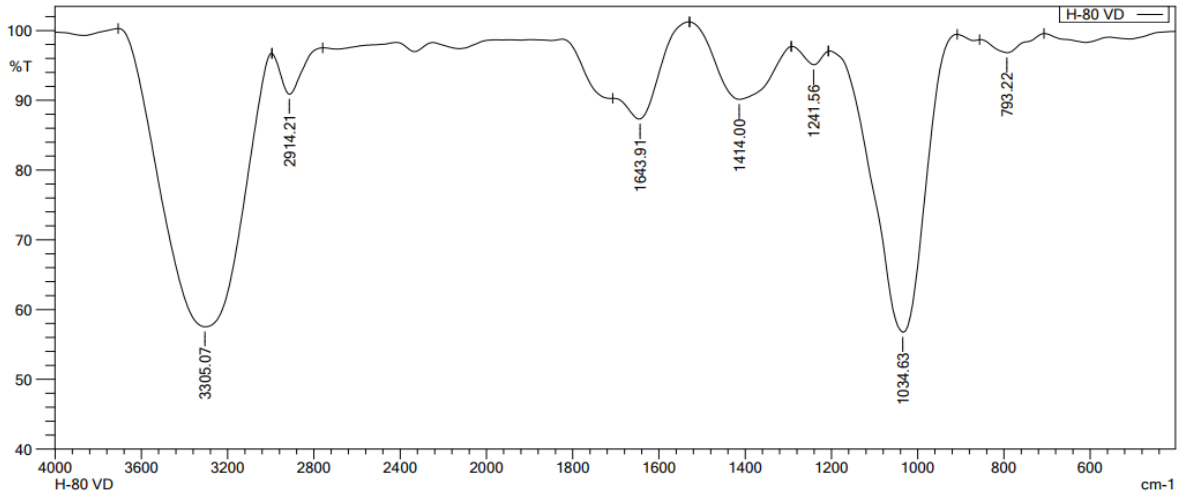

(c)

Figure 4. FTIR spectra of (a) the control sample (sample 1: 0% honey), (b) air-dry sample 5: 80% honey, and (c) vacuum-dry sample 5: 80% honey

Fourier Transform Infrared Spectroscopy (FTIR)

Figure 4(a) shows the FTIR spectra of the control sample (sample 1 with 0% honey), whilst Figures 4(b) and (c) depict the FTIR spectra of the air-dry and vacuum-dry honey-pectin hydrogel samples 5 with 80% honey, respectively. The decision to feature the spectra from sample 5 is based on the analysis of results obtained during this study, which indicated that although all honey-containing samples showed gradual changes in spectral features, sample 5 exhibited the most pronounced and distinct spectral alterations. These alterations are most representative of the impact of high honey concentrations on the hydrogel properties. To maintain clarity and focus in the spectral presentation and to avoid redundancy, spectra from samples with lower honey concentrations, which showed similar but less pronounced changes, are not displayed separately. This selective representation allows for a clearer demonstration of the significant spectral differences and interactions facilitated by the highest honey content.

The FTIR spectrum for the hydrogel with no honey exhibits distinct peaks at 3642 cm^{-1}, indicative of free hydroxyl (O-H) groups, and at 1749 cm^{-1} for carbonyl (C=O) groups typically found in ester or carboxylic acid forms [32]. The peak at 1454 cm^{-1} is suggested as –CH scissoring on pectin compound [33]. Peak at 1130 cm^{-1} likely represents C-O stretching vibrations found in ether and alcohol groups, common in polysaccharides like pectin, whereas peak at 1023 cm^{-1} is suggested as –CH–O–CH– stretching [34].

The addition of honey markedly influences the FTIR spectrum of the hydrogel, with the spectrum showcasing a notable broad band at 3316.6 cm^{-1} which indicates extensive hydrogen bonding, a characteristic that underscores the strong interaction facilitated by honey within the hydrogel matrix. Additionally, a distinct peak at 1034.6 cm^{-1} is observed, attributed to the presence of the C-O-C group in honey [16,17]. Other significant but smaller peaks include 2914 cm^{-1} for C-H stretching, 1643 cm^{-1} for C=C stretching typically linked to unsaturated groups, and 1414 cm^{-1} which might represent additional O-H bending vibrations [35]. These peaks indicate a more ordered arrangement of molecular interactions within the hydrogel. The presence of honey possibly changes the degree of cross-linking within the hydrogel by introducing additional hydroxyl groups that interact with the galacturonic acid components of pectin. These interactions facilitate a denser network of hydrogen bonds, enhancing the structural integrity of the hydrogel. This is evidenced by the sharper and more distinct IR spectral peaks, which signify a more orderly arrangement of molecular interactions and an overall stabilization of the hydrogel matrix.

The FTIR spectrum of the vacuum-dried hydrogel closely aligns with that of the air-dried sample, with minor adjustments indicative of the influence of the drying technique on the hydrogel's molecular structure. Like its air-dried counterpart, the vacuum-dried sample prominently displays peaks at 3305 cm^{-1} for O-H groups, 1034.6 cm^{-1} for C-O-C group, and 2914 cm^{-1} for C-H stretching, underscoring the stability of these essential functional groups regardless of the drying method. Moreover, the peaks associated with C=C double bonds and additional O-H groups (observed at 1643 cm^{-1} and 1414 cm^{-1}, respectively) appear with similar prominence as in the air-dried samples, suggesting that the fundamental honey-pectin interactions are maintained even under the more stringent conditions of vacuum drying. A particularly interesting feature in the vacuum-dried sample is the emergence of a small new peak at 793 cm^{-1} might indicate the potential formation of new crystalline structures or the initiation of unique molecular interactions, which could be facilitated by the specific conditions of vacuum drying—namely, reduced pressure and the absence of ambient moisture. It is hypothesized that such structural changes might influence the hydrogel’s mechanical properties or its bioactive behavior. However, these potential effects are speculative at this stage and require further experimental validation. Future studies should focus on elucidating the precise nature of these interactions and their implications for the hydrogel's functionality in specific applications.

It is important to elucidate the inherent properties of pectin and their impact on its spectral appearance. Pectin, a polysaccharide derived from plant cell walls, primarily consists of galacturonic acid units. The spectral characteristics of pectin can vary significantly depending on its degree of esterification and methylation. High degrees of methylation typically result in broader, less intense IR absorbance peaks due to the distribution and density of methoxyl groups, which can obscure distinct peak formations. However, it is recognized that under optimal conditions, pectin can exhibit well-defined IR spectra, as evidenced by existing literature [36] demonstrating detailed vibrational features. It is important to clarify that the variability in the spectral quality observed in our studies was not solely due to the inherent properties of pectin but also influenced by the analytical conditions and the interaction with honey.

When examining the FTIR spectra, notable differences are evident between samples with and without honey. The control spectrum, containing only pectin, exhibits a complex pattern reflecting a broad array

of loosely associated functional groups. This complexity corresponds with the less cohesive structural formations observed via SEM. Conversely, spectra from honey-enriched samples display clearer and more distinct peaks, suggesting that the addition of honey may stabilize and enhance the organization within the hydrogel matrix. These spectral improvements in honey-enriched samples may be attributed to honey acting as a plasticizer, which facilitates a more uniform distribution of functional groups and enhances the overall structural integrity of the hydrogel.

Both the air-dried and vacuum-dried samples with honey exhibit these characteristics, although subtle variations exist. For instance, vacuum-dried samples with honey occasionally demonstrate additional peaks at lower wavenumbers, which could be indicative of specific molecular changes enhanced by the drying conditions. These distinctions suggest that while honey fundamentally simplifies and stabilizes the molecular structure of the hydrogels, the chosen method of drying can further modulate these interactions, potentially enhancing the material's stability and functional performance in practical applications. Such nuances in spectral presentation and structural observations underscore the importance of both composition and processing methods in designing effective hydrogel formulations for biomedical use.

This observed homogeneity in the FTIR spectra, particularly in honey-enriched hydrogels, correlates well with the SEM observations, where increasing honey content leads to more defined network structures in the hydrogels. This is indicative of the synergistic interaction between honey and pectin, improving both the structural and spectral properties of the hydrogels. Furthermore, these interaction effects may alter the visibility and intensity of certain characteristic peaks of pectin, as demonstrated in our analyses. The preparation methods, including varying concentrations, mixing procedures, and curing conditions, are crucial in achieving these results, highlighting the importance of both composition and processing methods in the design of effective hydrogel formulations for potential biomedical applications.

The emergence of new peaks in the vacuum-dried sample, absent in the air-dried counterpart, highlights the role of the drying process in influencing the structural configuration and chemical interactions within the hydrogel. SEM analysis supports this, showing that air-dried hydrogels exhibit more compact and less disintegrated layers compared to vacuum-dried hydrogels. The formation of these new FTIR peaks could be attributed to tighter molecular packing or new crystalline structures, likely a result of the lower moisture environment and higher temperatures associated with air drying. This suggests that the drying method plays a crucial role in defining the hydrogel’s chemical characteristics and mechanical stability, enhancing the material's integrity for practical applications.

While FTIR spectroscopy has provided valuable insights into the structural and chemical properties of the hydrogels, the potential benefits of integrating Raman spectroscopy for a more comprehensive analysis cannot be more emphasised. Additionally, the absence of control spectra for honey and spectra with a low honey to pectin ratio in our initial study was noted. Future studies will aim to incorporate these elements to provide a clearer differentiation of the spectral contributions of each component and to further elucidate the unique features present only in the composites compared to the individual components.

Swelling Ratio Analysis

Figure 5 provides a detailed visual analysis of the swelling behavior of hydrogel samples through interpolated line plots that delineate swelling kinetics across varying honey concentrations. For a more comprehensive overview of the data, readers are directed to Table A1 in Appendix A. The plots systematically categorize samples 1-5, representing hydrogels with increasing volumes of honey—from sample 1, the control with 0% honey, to sample 5, which contains the highest concentration. The composition details for each sample are explicitly outlined in Table 1.

These plots are meticulously designed to illustrate the progression of swelling over time, effectively highlighting the distinct responses between air-dried and vacuum-dried samples. The use of interpolation in these plots not only emphasizes underlying trends but also enhances the clarity of swelling dynamics. This approach facilitates immediate visual comparison and assists in identifying subtle patterns and dynamics within the swelling process that may not be readily apparent from the tabulated data alone. Curve-fitting techniques were applied to quantify swelling behavior; with summary of fitted models and R^2 values presented in Table 2. These fitted equations provide a quantitative assessment of each hydrogel sample’s swelling pattern, offering insights into the moisture retention properties of the hydrogels. The high R^2 values (all above 0.95) indicate strong agreement with the fitted models, reinforcing the characteristic swelling trends observed.

Table 2. Summary of fitted equations and R^2 values for swelling ratio analysis

Hydrogel Sample	Fitted Equation	R^2 Value
Sample 1	$y = 2.0052 - 1.3509.e^{-0.0437x}$	0.9943
Sample 2, Air Dry	$y = 1.8328 - 0.8059.e^{-0.0866x}$	0.9984
Sample 2, Vac Dry	$y = 2.1063 - 1.2693.e^{-0.0457x}$	0.9869
Sample 3, Air Dry	$y = 2.1716 - 0.4965.e^{-0.1108x}$	0.9917
Sample 3, Vac Dry	$y = 2.4620 - 0.5764.e^{-0.0760x}$	0.9721
Sample 4, Air Dry	$y = 2.0385 - 0.4149.e^{-0.1049x}$	0.9842
Sample 4, Vac Dry	$y = 1.7948 - 0.3184.e^{-0.1435x}$	0.9902
Sample 5, Air Dry	$y = -0.0011x^2 + 0.0286x + 2.2325$	0.9802
Sample 5, Vac Dry	$y = -0.0008x^2 + 0.0273x + 1.8370$	0.9584

Note: The 80% honey air-dried and vacuum-dried hydrogels follow a polynomial (quadratic) model, rather than an exponential decay trend, due to its distinct swelling characteristics. However, the high R^2 values (0.98 and 0.95) confirm the robustness of this fit.

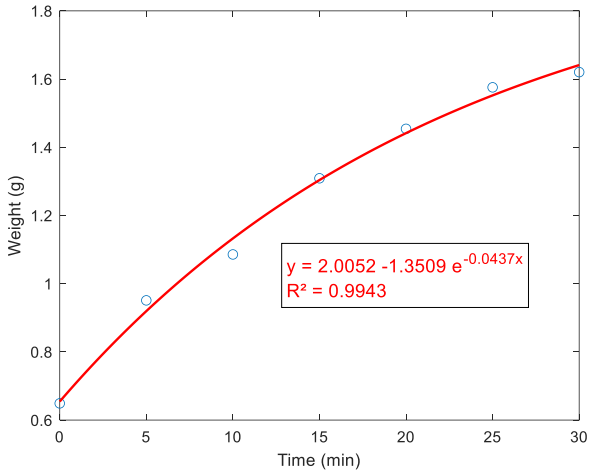

(a)

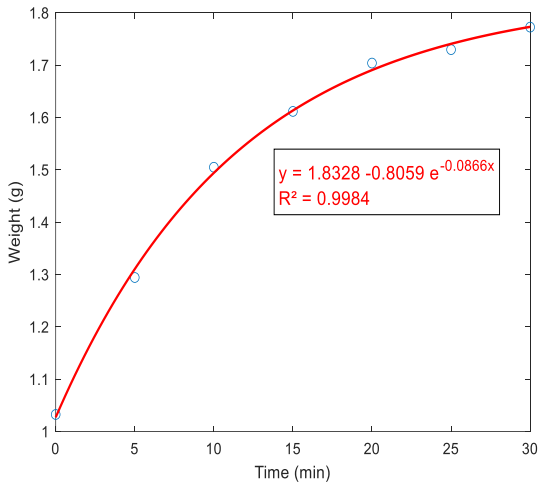

(b)

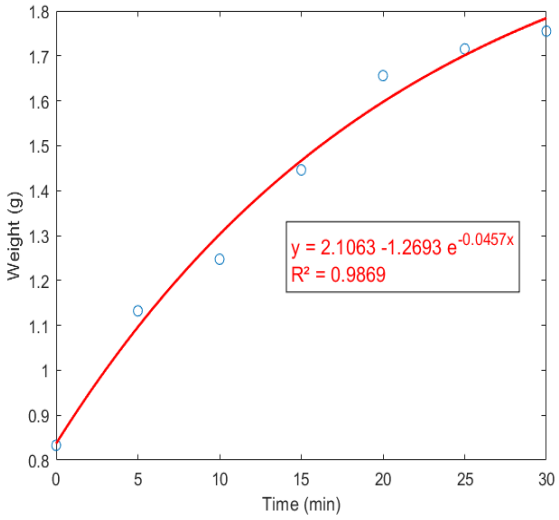

(c)

Continue to next page

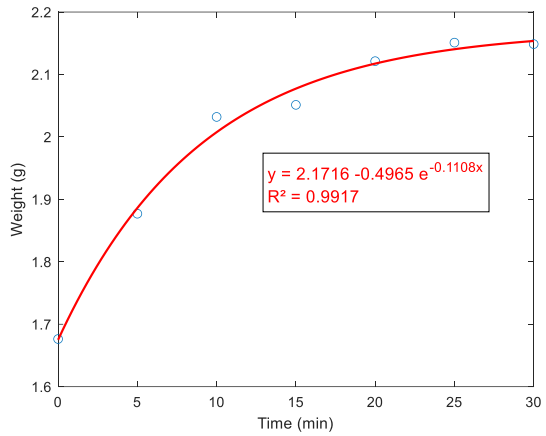

(d)

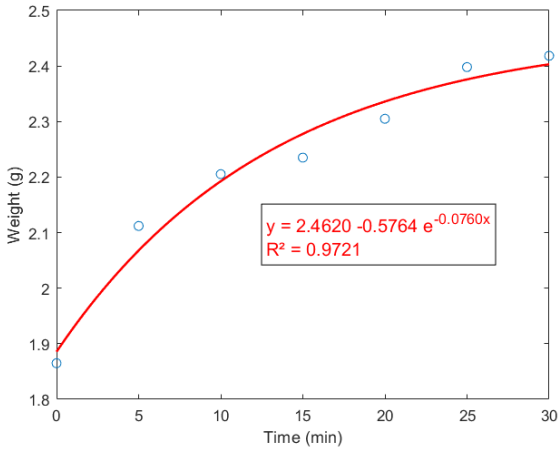

(e)

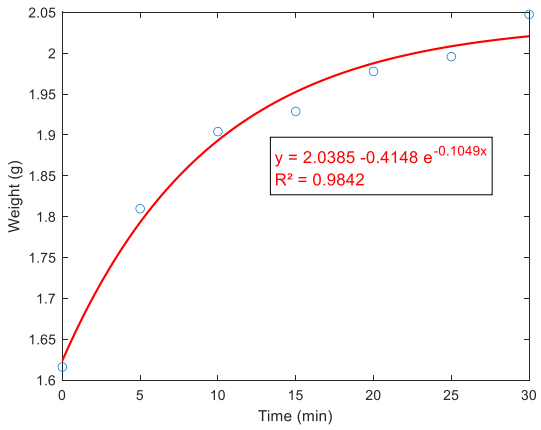

(f)

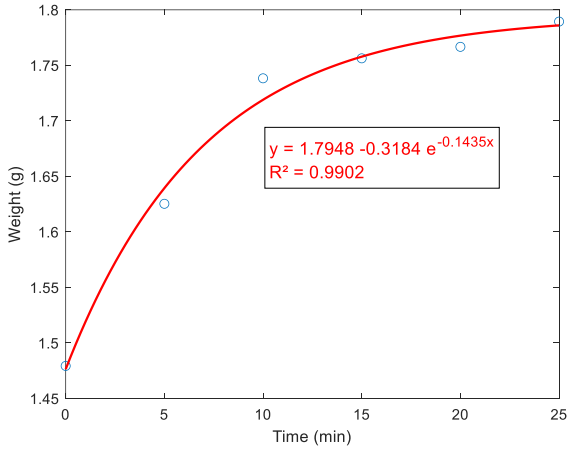

(g)

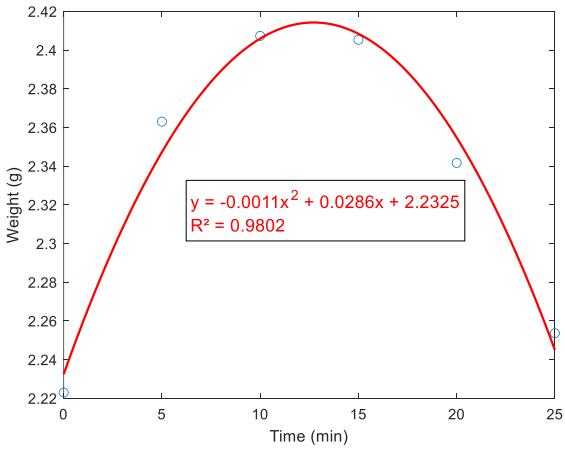

(h)

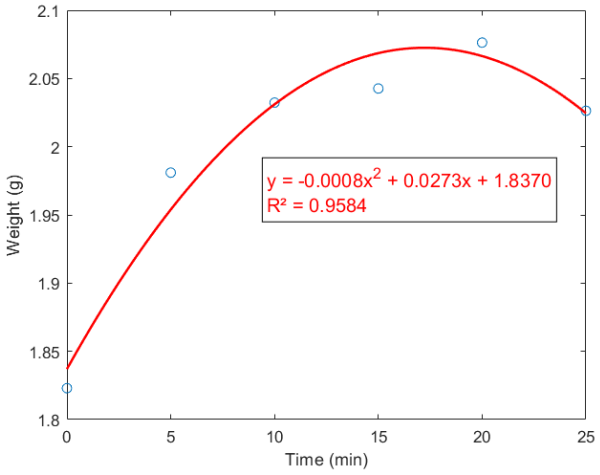

(i)

Figure 5. Time progression of average weight of the hydrogel in the swelling analysis test for (a) sample 1, (b) sample 2 – air dry, (c) sample 2 – vacuum dry, (d) sample 3 – air dry, (e) sample 3 – vacuum dry, (f) sample 4 – air dry, (g) sample 4 – vacuum dry, (h) sample 5 – air dry, and (i) sample 5 – vacuum dry

It can be seen that generally the hydrogel samples exhibited a characteristic logarithmic increase in weight over time, a behavior primarily driven by the water absorption dynamics of the hydrogel matrix. This logarithmic pattern is indicative of the osmotic pressure differences between the polymer structure and the surrounding phosphate-buffered saline (PBS), which simulates the wound environment. Initially, water uptake is rapid due to the high availability of hydrophilic sites within the polymer network, facilitating swift absorption. This rapid uptake phase aligns with findings by Giusto *et al*. [27,28], where the hydrogel samples demonstrated a significant increase in fluid content, underscoring the capability of the hydrogels to prevent fluid buildup when used on wounds. This is promising because it indicates the hydrogel's potential effectiveness in managing wound exudate, which is crucial for promoting healing and preventing complications like infections. As the hydrogel swells, these sites become increasingly saturated, and the internal structure of the hydrogel expands, reducing the effective concentration gradient and increasing the mechanical resistance against further swelling. This results in a decreasing rate of water absorption, manifesting as a logarithmic trend. This behavior is particularly advantageous in wound care applications, where a quick initial uptake of moisture is crucial for maintaining an optimal moist environment that promotes healing, followed by a stable state that prevents oversaturation and potential leakage.

The present study extends the observations made by Giusto *et al*. [27,28] by quantitatively analyzing how varying concentrations of honey affect these absorption dynamics, offering new insights into optimizing hydrogel formulations for specific therapeutic requirements. This nuanced understanding of hydrogel behavior under different formulation ratios provides valuable information for tailoring hydrogel properties to meet diverse clinical needs.

Interestingly, the hydrogel with 80% honey concentration demonstrates an intriguing polynomial swelling behavior, characterized by an initial increase followed by a slight decrease in weight. This initial increase in weight can be primarily attributed to the hygroscopic nature of honey at high concentrations, which enhances water absorption at the initial stage. However, the subsequent reduction in weight suggests structural compromises, possibly due to the mechanical integrity of the hydrogel being unable to withstand the stresses induced by excessive swelling. This phenomenon, known as syneresis, involves the contraction of the hydrogel matrix and the expulsion of absorbed water, indicating a breakdown in the structural stability of the material. Moreover, this behavior may be exacerbated by the reversal of osmotic pressure within the highly saturated hydrogel. As the internal network begins to degrade under stress, the osmotic forces that initially drove water absorption may reverse, actively driving the expulsion of water from the hydrogel. This observation, while consistent with some hydrogel behaviors in response to external stimuli such as pH and temperature changes, as documented in the literature [37,38], suggests a unique interaction within our honey-enriched hydrogel system that could be further investigated.

The theoretical deductions regarding the impact of honey saturation on hydrogel stability are speculative at this stage and not yet supported by direct experimental evidence. Future studies should focus on elucidating the precise nature of these interactions and their implications for the hydrogel's functionality in specific applications, possibly employing techniques such as UV/vis spectroscopy [39]to measure honey extraction and advanced spectroscopic analyses to understand the molecular interactions at play. These studies will help to determine whether the observed changes are due to honey extraction or other structural degradation mechanisms, providing a clearer understanding of the material's behavior under various physiological conditions.

These findings underscore the importance of optimizing hydrogel formulations based on their intended applications. The ability to tailor the drying process and adjust honey concentrations impacts not only the hydrogel’s swelling efficiency but also its structural and functional efficacy in practical applications. This detailed understanding of the hydrogel's swelling dynamics and the interplay between its composition and structural properties is invaluable for designing next-generation hydrogel products tailored for specific medical and therapeutic fields, ensuring precise control over moisture management and material stability.

Complementing these general observations, Table 3 presents the derived swelling ratios, highlighting significant variations influenced by both the drying methods and the concentrations of honey. Notably, the control sample, which lacks honey, consistently demonstrates a superior swelling capacity relative to the honey-pectin hydrogels. This enhanced capacity can be attributed primarily to the absence of denser network structures that are typically reinforced by honey-pectin interactions (see Figure 2). The reduced network density in the control samples allows for more extensive liquid diffusion throughout the matrix, thereby facilitating a higher swelling ratio. Such a characteristic underscores the potential of the control gel in applications where rapid and substantial fluid uptake is crucial, such as in highly exudative wound environments.

Furthermore, hydrogel samples subjected to vacuum drying generally exhibit higher swelling ratios compared to their air-dried counterparts. This observation suggests that vacuum drying techniques help in preserving the hydrogel's inherent porous structure more effectively. By minimizing the collapse of pores during the drying process, vacuum drying enhances the overall water absorption capacity of the hydrogels. This preservation of porosity is crucial for maintaining the hydrogel's functionality, especially in medical applications where consistent moisture management is required.

The absorption rate of the hydrogel samples was notably higher in sample number 2, which was subjected to vacuum drying, indicating the beneficial effects of this drying method on fluid uptake. However, as the content of the honey was further increased in samples 3, 4, and 5—with 40 ml, 60 ml, and 80 ml of honey, respectively—the swelling ratio of the hydrogels decreased. This decrease can be attributed to the cross-linking reactions between honey and pectin, which lead to the formation of denser network structures as evidenced in Figure 3. The SEM images show that the higher the honey content, the tighter the matrix networks are, restricting the space available for liquid diffusion and thus reducing the swelling capacity. This pattern of results aligns with findings reported by Ma *et al*. [40], where similar trends were observed. Additionally, despite the higher initial absorption rates in vacuum-dried hydrogels, increasing honey concentrations generally led to decreased swelling ratios, underscoring the complex interplay between hydrogel composition, drying method, and swelling behavior.

Table 3. The swelling ratio of the control and honey-pectin hydrogels

Time (min)	Sample 1	Sample 2		Sample 3		Sample 4		Sample 5	
	Control	Air Dry	Vac Dry	Air Dry	Vac Dry	Air Dry	Vac Dry	Air Dry	Vac Dry
5	46.53 ± 0.76	25.35 ± 0.52	35.88 ± 5.83	11.97 ± 0.08	13.24 ± 0.86	11.98 ± 1.41	9.87 ± 1.24	6.30 ± 2.02	8.67 ± 0.54
10	67.28 ± 0.81	45.75 ± 0.56	49.68 ± 2.44	21.22 ± 0.21	18.25 ± 4.86	17.82 ± 2.67	17.51 ± 0.32	8.29 ± 2.49	11.48 ± 3.65
15	101.69 ± 0.62	56.09 ± 0.59	73.52 ± 7.75	22.37 ± 0.12	19.84 ± 6.01	19.35 ± 1.69	18.72 ± 0.82	8.20 ± 0.45	12.05 ± 3.48
20	124.04 ± 4.47	65.03 ± 0.48	98.72 ± 10.57	26.55 ± 0.14	23.59 ± 6.64	22.38 ± 0.07	19.42 ± 4.49	5.34 ± 2.62	13.90 ± 0.96
25	142.78 ± 2.70	67.52 ± 0.56	105.86 ± 8.04	28.32 ± 1.03	28.58 ± 2.19	23.49 ± 1.59	20.96 ± 6.73	1.38 ± 4.01	11.15 ± 0.46
30	149.67 ± 4.29	71.68 ± 0.62	110.60 ± 7.19	28.18 ± 1.03	29.67 ± 1.65	26.70 ± 0.43	-	-	-

The absorption rate and swelling behaviors observed in the hydrogel samples provide critical insights into their capacity for moisture management capabilities, which are essential for effective wound dressings. As the content of honey increased in samples 3, 4, and 5, leading to a decreased swelling ratio due to denser network structures, there is a notable impact on the Hydrogel Dehydration Rate Testing (HDRT). HDRT is crucial in wound care as it measures the ability of a dressing to release moisture under controlled conditions, reflecting how well the dressing can manage the moisture environment at the wound site. An ideal hydrogel dressing should balance its dehydration rate to prevent excess moisture that can foster bacterial growth, while retaining sufficient moisture to promote healing processes.

Hydrogel Dehydration Rate Testing (HDRT)

Figure 6 illustrates the weight progression of the hydrogel samples over time during the Hydrogel Dehydration Rate Testing (HDRT), categorized by different drying methods and varying concentrations of honey. To better characterize the moisture loss dynamics, exponential regression models were applied to fit the dehydration trends of the hydrogel samples. On the other hand, a polynomial (quadratic) model was used for the 80% honey vacuum-dried sample instead, as it exhibited a deviation from the typical exponential behaviour. The interpolation provides a detailed visual representation of how each hydrogel sample responds to the conditions of the HDRT, smoothing the data to highlight the dynamic changes in weight that reflect their dehydration characteristics. The summary of fitted models and R^2 values is presented in Table 4.

By employing these curve-fitting techniques, Figure 6 provides a quantitative assessment of each hydrogel sample's dehydration pattern. The fitted equations, along with their R^2 values, quantify the strength of the correlation between weight reduction and time, offering a deeper understanding of the hydrogels' water vapor transmission rate (WVTR). The high R^2 values (all above 0.95) indicate strong

agreement with the fitted models. These reinforce the characteristic exponential weight loss trend associated with efficient moisture transmission.

This trend is consistent across almost all samples; exhibiting a characteristic exponential decrease in weight over the test period, which indicates effective moisture release capabilities. The observed weight reduction suggests that the hydrogels are actively transmitting water vapor. Maintaining this property is essential for optimal moisture conditions in wound care, as it directly correlates to WVTR by demonstrating the hydrogel's ability to release moisture to the environment. However, a notable exception is observed in the hydrogel with 80% honey concentration, particularly in the vacuum-dried variant, where the weight reduction pattern deviates from the exponential trend. The best-fit quadratic model for this sample suggests that higher honey concentrations may alter the hydrogel's structural properties at higher honey concentrations, potentially impacting its ability to regulate moisture effectively. Despite this deviation, the model still exhibits a high R^2 values (>0.95), indicating a strong correlation.

Table 4. Summary of fitted equations and R^2 values for hydrogen dehydration rate testing

Hydrogel Sample	Fitted Equation	R^2 Value
Sample 1	$y = 0.9359 + 0.0772.e^{-0.0255x}$	0.9798
Sample 2, Air Dry	$y = 1.7891 + 0.2321.e^{-0.0194x}$	0.9962
Sample 2, Vac Dry	$y = 1.5887 + 0.0653.e^{-0.0343x}$	0.9931
Sample 3, Air Dry	$y = 2.8959 + 0.3851.e^{-0.0071x}$	0.9868
Sample 3, Vac Dry	$y = 3.0094 + 0.1985.e^{-0.0132x}$	0.9970
Sample 4, Air Dry	$y = 2.9535 + 0.2354.e^{-0.0204x}$	0.9902
Sample 4, Vac Dry	$y = 2.6985 + 0.1887.e^{-0.0088x}$	0.9865
Sample 5, Air Dry	$y = 3.4192 + 0.2538.e^{-0.0172x}$	0.9793
Sample 5, Vac Dry	$y = 0.00x^2 - 0.0016x + 3.4888$	0.9509

Note: The 80% honey vacuum-dried hydrogel follows a polynomial (quadratic) model, rather than an exponential decay trend, due to its distinct dehydration characteristics. However, the high R^2 value (0.95) confirms the robustness of this fit.

Table 5 summarizes the dehydration rate values over a 3-hour period for the different samples, revealing significant variation influenced by both drying methods and honey content. Interestingly, despite the SEM and FTIR analyses indicating a more compact structure in air-dried hydrogels, their dehydration rate ranged significantly from 37.24 to 50.02 g/m²/h, which is notably higher than the control sample's rate of approximately 14.54 g/m²/h. This counterintuitive finding underscores the complexity of hydrogel behavior, suggesting that while the air-dried samples are more compact, they may still offer efficient pathways for moisture transmission.

Conversely, the vacuum-dried hydrogels displayed lower dehydration rates, ranging from minimal to moderate levels i.e. from 11.03 to 31.58 g/m²/h. Despite an overall decrease compared to air-dried samples, some vacuum-dried samples showed an increase in dehydration rate compared to the control. This suggests that while vacuum drying typically results in a denser structure, reducing dehydration rate, certain formulation adjustments, such as the concentration of honey, can moderate this effect.

The variation in dehydration rates across different samples and treatments emphasizes the complex interplay between hydrogel composition, structure, and drying method. Although vacuum-dried Sample 2 exhibits a notably lower dehydration rate at 11.03 g/m²/h, suggesting reduced efficacy in moisture management, other vacuum-dried samples manage to achieve higher rates, demonstrating that appropriate formulation and processing adjustments can optimize moisture management. These findings align well with the literature, particularly by Valipour *et al*. [41], who reported that WVTR varies with the content of dialdehyde starch (DAS) in hydrogels. Despite our study primarily measuring HDRT instead

of traditional methods that measure water loss through the entire test setup over extended periods [41]. Instead, the focus is on direct measurement of dehydration in the hydrogels themselves, under controlled conditions, to accurately monitor changes in water content. This method elucidates the intrinsic dehydration characteristics of hydrogels, crucial for applications requiring precise moisture management. By assessing the direct water content changes in hydrogels, a focused understanding of their performance is obtained, complementing broader WVTR assessments in the literature. This connection reinforces the relevance of our findings to existing knowledge on hydrogel behavior, suggesting that variations in hydrogel components can profoundly affect their ability to manage moisture, a critical factor for their efficacy in wound care applications.

This comprehensive analysis provides a robust foundation for understanding and optimizing hydrogel dressings for wound care. The data not only reinforces the importance of carefully choosing hydrogel components and drying methods but also opens avenues for further research into how these variables can be fine-tuned to meet specific clinical requirements. Future studies could explore more diverse formulations or innovative drying techniques to further enhance the functional properties of hydrogel dressings, ensuring they meet the precise needs of modern wound management. These investigations will continue to refine the understanding of hydrogel behavior, particularly under varying environmental conditions, enhancing their practical application in medical settings.

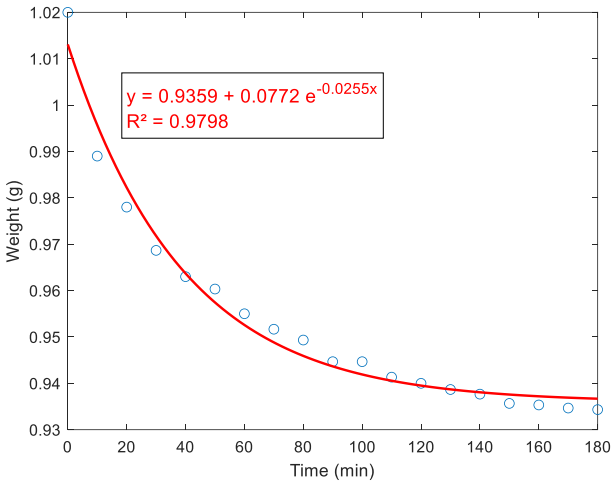

(a)

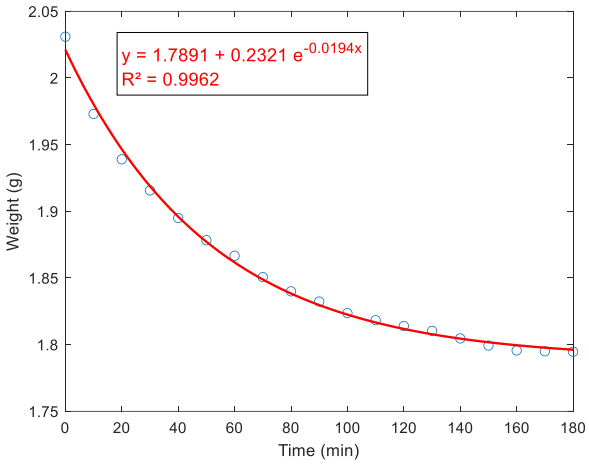

(b)

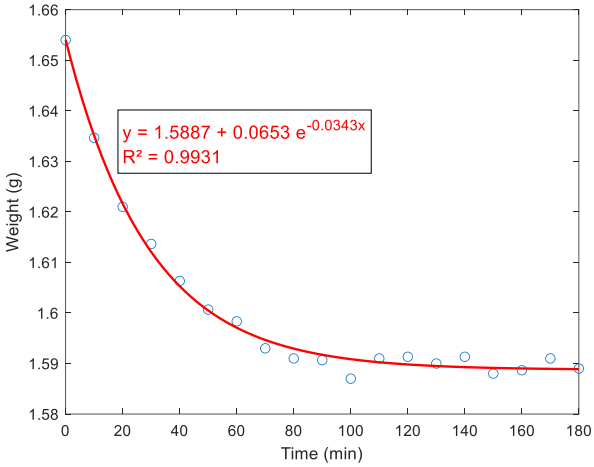

(c)

Continue to next page

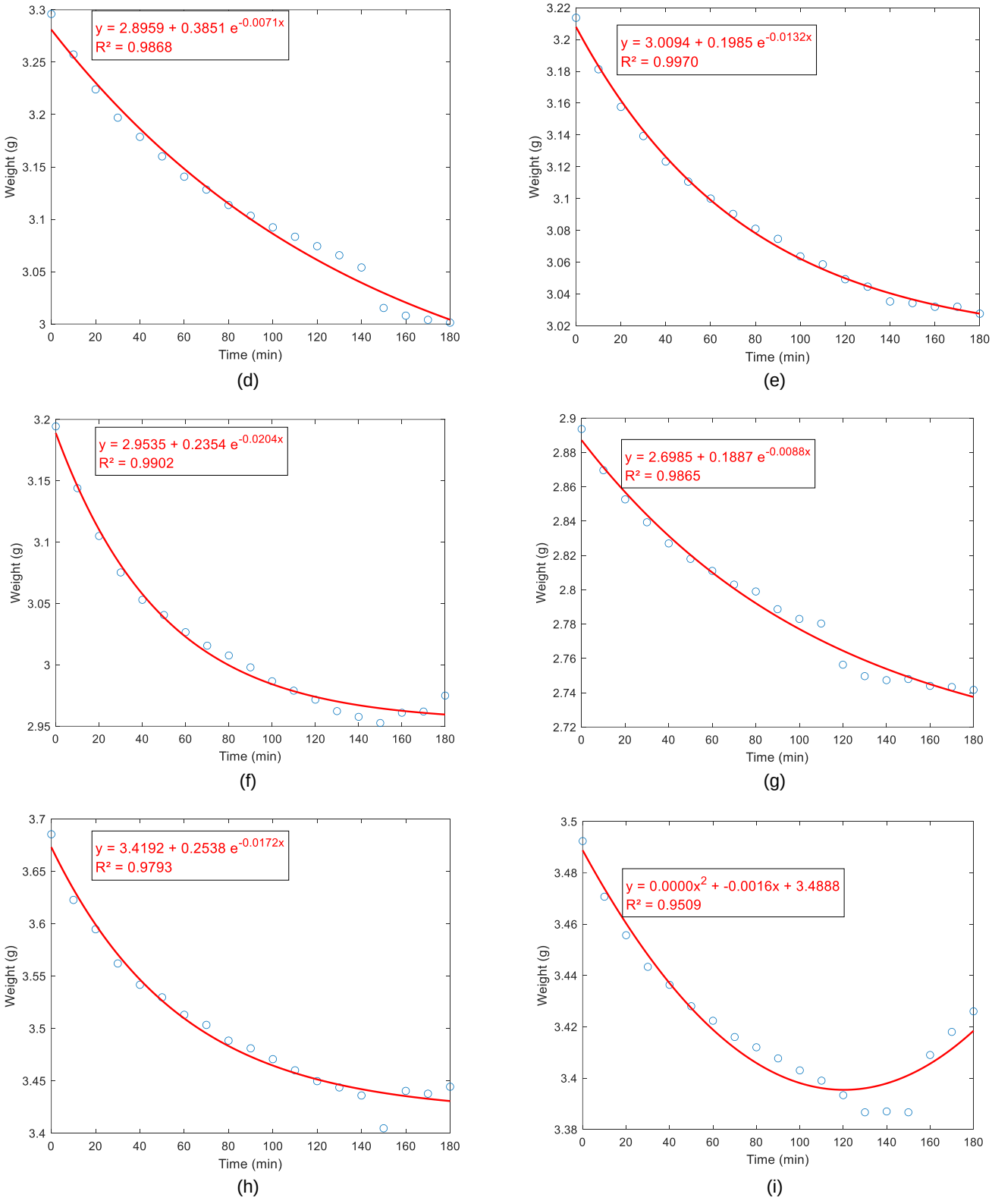

Figure 6. Time Progression of average weight of the hydrogel in the hydrogel dehydration rate testing (HDRT) for (a) sample 1, (b) sample 2 – air dry, (c) sample 2 – vacuum dry, (d) sample 3 – air dry, (e) sample 3 – vacuum dry, (f) sample 4 – air dry, (g) sample 4 – vacuum dry, (h) sample 5 – air dry, and (i) sample 5 – vacuum dry

Table 5. The hydrogel dehydration rate testing (HDRT) of the control and honey-pectin hydrogels

Time	Sample 1	Sample 2		Sample 3		Sample 4		Sample 5	
	Control	Air Dry	Vac Dry	Air Dry	Vac Dry	Air Dry	Vac Dry	Air Dry	Vac Dry
3 h	14.54 ± 1.19	40.12 ± 2.63	11.03 ± 3.73	50.02 ± 0.72	31.58 ± 6.36	37.24 ± 3.56	25.8 ± 5.80	40.91 ± 2.04	11.26 ± 4.56

Conclusions

This study was motivated by the need for effective wound dressings that can maintain a moist healing environment, support cellular activities, and prevent infections. Utilizing natural polymer, namely pectin, and honey, this research developed hydrogels through the solution casting method aimed at optimizing wound healing mechanisms. The choice of honey, specifically, stingless bee honey, and pectin was based on their well-documented properties in promoting wound repair due to their biocompatibility, bioactivity, and moisture retention capabilities, as well as the availability and popularity of stingless bee honey in the region.

The synthesis process was methodically detailed to ensure reproducibility and consistency across different hydrogel formulations. Various concentrations of honey were explored to understand its impact on the hydrogel properties, with a systematic approach to characterizing these variations through Scanning Electron Microscopy (SEM), Fourier Transform Infrared Spectroscopy (FTIR), Swelling Test, and Hydrogel Dehydration Rate Testing (HDRT) Analysis. Key findings from the study highlighted that hydrogels with optimized honey concentrations provide significant improvements in structural integrity and chemical stability, as evidenced by SEM and FTIR results. These hydrogels exhibited effective swelling behavior and moisture management, which are crucial for maintaining a conducive wound healing environment. Specifically, air-dried hydrogels showed higher water vapor transmission rates compared to vacuum-dried samples, suggesting that air-drying techniques might better preserve the functional properties needed for wound dressing applications. It is important to recognize that while the inherent properties of pectin influence its spectral appearance, high-quality IR spectra can be obtained under optimal conditions, as established in the literature [36]. Future analyses will therefore focus on optimizing these conditions to improve spectral quality and on using Raman spectroscopy to complement the findings from IR spectroscopy.

The significance of these findings lies in their contribution to the development of more effective wound dressing materials that can adaptively manage moisture levels, promote faster healing, and potentially reduce the risk of infection. The incorporation of honey not only enhances the structural and mechanical properties of the hydrogels but also contributes to their therapeutic effectiveness.

Moving forward, this research opens avenues for further optimization of the hydrogel formulations. Additional studies could focus on integrating antimicrobial agents or other therapeutic substances to enhance the bioactivity and mechanical strength of the hydrogels. This will include rigorous evaluations of antibacterial efficacy, antioxidant capacity, and the assessment of mechanical properties such as tensile modulus, ultimate tensile stress, and ultimate strain to ensure the hydrogels meet the rigorous demands of clinical settings. Furthermore, the cytocompatibility of these hydrogels will be assessed using standard assays such as MTT and XTT on cells involved in the wound healing process, providing crucial insights into their suitability for direct application on wounds. Our future investigation will also extend to analyzing the swelling behavior of the hydrogel samples using a UV-Vis spectrophotometer to better understand their ability to maintain moisture and facilitate drug delivery in a controlled manner. Long-term clinical trials are also recommended to validate the efficacy and safety of these hydrogel dressings in a real-world medical setting. Ensuring the feasibility of this hydrogel as a wound healing material will also require comprehensive testing such as the anti-bacterial and biocompatibility tests. Such tests will provide a more comprehensive evaluation of the hydrogel's safety and efficacy, ensuring it meets the necessary standard for clinical application in wound healing.

Additionally, exploring scale-up production and assessing the economic feasibility of these hydrogels will be crucial for their commercialization and wider adoption in healthcare settings. By extending the research to include these vital evaluations, we aim to develop hydrogels that not only meet the physical requirements for wound dressings but also actively contribute to the healing process through biofunctional capabilities. These advancements will be instrumental in transitioning from laboratory research to clinical application, ensuring that the hydrogels are both safe and effective for managing wounds in diverse medical environments.

Conflicts of Interest

The authors declare that there is no conflict of interest regarding the publication of this paper.

Acknowledgement

This research and the APC were funded by Universiti Brunei Darussalam Research Grant No.: UBD/RSCH/1.3/FICBF(b)/2020/005.

References

[1] Zahra, D., *et al.* (2023). Exploring the recent developments of alginate silk fibroin material for hydrogel wound dressing: A review. *International Journal of Biological Macromolecules, 248*, 125989. https://doi.org/10.1016/j.ijbiomac.2023.125989

[2] IDF Diabetes Atlas. (2022). *IDF Diabetes Atlas 2022 Reports*.

[3] Iranmanesh, N., *et al.* (2024). Improving trauma patient management: Predisposing factors for trauma-induced physiological disorders and the importance of damage control surgery. *Current Problems in Surgery, 61*(6), 101473. https://doi.org/10.1016/j.cpsurg.2024.101473

[4] Yasin, S. N. N., Said, Z., Halib, N., Rahman, Z. A., & Mokhzani, N. I. (2023). Polymer-based hydrogel loaded with honey in drug delivery system for wound healing applications. *Polymers, 15*(14), 3085. https://doi.org/10.3390/polym15143085

[5] Xiang, J., Shen, L., & Hong, Y. (2020). Status and future scope of hydrogels in wound healing: Synthesis, materials and evaluation. *European Polymer Journal, 130*, 109609. https://doi.org/10.1016/j.eurpolymj.2020.109609

[6] Hu, Y. Y. (2015). A review on antimicrobial silver absorbent wound dressings applied to exuding wounds. *Journal of Microbial & Biochemical Technology, 7*(4). https://doi.org/10.4172/1948-5948.1000212

[7] Cullen, B., & Gefen, A. (2023). The biological and physiological impact of the performance of wound dressings. *International Wound Journal, 20*(4), 1292–1303. https://doi.org/10.1111/iwj.13960

[8] Zhang, S., *et al.* (2023). Polysaccharide-based hydrogel promotes skin wound repair and research progress on its repair mechanism. *International Journal of Biological Macromolecules, 248*, 125949. https://doi.org/10.1016/j.ijbiomac.2023.125949

[9] Firlar, I., Altunbek, M., McCarthy, C., Ramalingam, M., & Camci-Unal, G. (2022). Functional hydrogels for treatment of chronic wounds. *Gels, 8*(2), 127. https://doi.org/10.3390/gels8020127

[10] Thomas, D. C., Tsu, C. L., Nain, R. A., Arsat, N., Fun, S. S., & Lah, N. A. S. N. (2021). The role of debridement in wound bed preparation in chronic wound: A narrative review. *Annals of Medicine and Surgery, 71*, 102876. https://doi.org/10.1016/j.amsu.2021.102876

[11] Zeng, D., Shen, S., & Fan, D. (2021). Molecular design, synthesis strategies and recent advances of hydrogels for wound dressing applications. *Chinese Journal of Chemical Engineering, 30*, 308–320. https://doi.org/10.1016/j.cjche.2020.12.005

[12] Holbert, M. D., *et al.* (2019). Effectiveness of a hydrogel dressing as an analgesic adjunct to first aid for the treatment of acute paediatric thermal burn injuries: Study protocol for a randomised controlled trial. *Trials, 20*(1), 13. https://doi.org/10.1186/s13063-018-3057-x

[13] Krishani, M., Shin, W. Y., Suhaimi, H., & Sambudi, N. S. (2023). Development of scaffolds from bio-based natural materials for tissue regeneration applications: A review. *Gels, 9*(2), 100. https://doi.org/10.3390/gels9020100

[14] Kedir, W. M., Deresa, E. M., & Diriba, T. F. (2022). Pharmaceutical and drug delivery applications of pectin and its modified nanocomposites. *Heliyon, 8*(9), e10654. https://doi.org/10.1016/j.heliyon.2022.e10654

[15] Munarin, F., Tanzi, M. C., & Petrini, P. (2012). Advances in biomedical applications of pectin gels. *International Journal of Biological Macromolecules, 51*(4), 681–689. https://doi.org/10.1016/j.ijbiomac.2012.07.002

[16] Eivazzadeh-Keihan, R., *et al.* (2022). Recent advances on biomedical applications of pectin-containing biomaterials. *International Journal of Biological Macromolecules, 217*, 1–18. https://doi.org/10.1016/j.ijbiomac.2022.07.016

[17] Li, D. Q., *et al.* (2021). Pectin in biomedical and drug delivery applications: A review. *International Journal of Biological Macromolecules, 185*, 49–65. https://doi.org/10.1016/j.ijbiomac.2021.06.088

[18] Roman-Benn, A., *et al.* (2023). Pectin: An overview of sources, extraction and applications in food products, biomedical, pharmaceutical and environmental issues. *Food Chemistry Advances, 2*, 100192. https://doi.org/10.1016/j.focha.2023.100192

[19] Han, S. S., Ji, S. M., Park, M. J., Suneetha, M., & Uthappa, U. T. (2022). Pectin based hydrogels for drug delivery applications: A mini review. *Gels, 8*(12), 834. https://doi.org/10.3390/gels8120834

[20] Yaghoobi, R., Kazerouni, A., & Kazerouni, O. (2013). Evidence for clinical use of honey in wound healing as an anti-bacterial, anti-inflammatory anti-oxidant and anti-viral agent: A review.

[21] Ratnayake, A., Yasin, H. M., Naim, A. G., & Abas, P. E. (2023). Classification of subspecies of honey bees using convolutional neural network. In *2023 6th International Conference on Applied Computational Intelligence in Information Systems (ACIIS)* (pp. 1–6). https://doi.org/10.1109/ACIIS59385.2023.10367282

[22] Yilmaz, A. C., & Aygin, D. (2020). Honey dressing in wound treatment: A systematic review. *Complementary Therapies in Medicine, 51*, 102388. https://doi.org/10.1016/j.ctim.2020.102388

[23] Almasaudi, S. (2021). The antibacterial activities of honey. *Saudi Journal of Biological Sciences, 28*(4), 2188–2196. https://doi.org/10.1016/j.sjbs.2020.10.017

[24] Bucekova, M., Godocikova, J., Kohutova, L., Danchenko, M., Barath, P., & Majtan, J. (2023). Antibacterial activity and bee-derived protein content of honey as important and suitable complementary tools for the assessment of honey quality. *Journal of Food Composition and Analysis, 123*, 105610. https://doi.org/10.1016/j.jfca.2023.105610

[25] Khataybeh, B., Jaradat, Z., & Ababneh, Q. (2023). Anti-bacterial, anti-biofilm and anti-quorum sensing activities of honey: A review. *Journal of Ethnopharmacology, 317*, 116830. https://doi.org/10.1016/j.jep.2023.116830

[26] El-Kased, R. F., Amer, R. I., Attia, D., & Elmazar, M. M. (2017). Honey-based hydrogel: In vitro and comparative in vivo evaluation for burn wound healing. *Scientific Reports, 7*(1). https://doi.org/10.1038/s41598-017-08771-8

[27] Giusto, G., *et al.* (2018). Pectin-honey hydrogel: Characterization, antimicrobial activity and biocompatibility. *Biomedical Materials and Engineering, 29*(3), 347–356. https://doi.org/10.3233/BME-181730

[28] Giusto, G., Vercelli, C., Comino, F., Caramello, V., Tursi, M., & Gandini, M. (2017). A new, easy-to-make pectin-honey hydrogel enhances wound healing in rats. *BMC Complementary and Alternative Medicine, 17*(1), 266. https://doi.org/10.1186/s12906-017-1769-1

[29] Cerullo, A., *et al.* (2023). The effects of pectin–honey hydrogel in a contaminated chronic hernia model in rats. *Gels, 9*(10), 811. https://doi.org/10.3390/gels9100811

[30] Suhaimi, H., & Das, D. B. (2016). Glucose diffusion in tissue engineering membranes and scaffolds. *Reviews in Chemical Engineering, 32*(6), 629–650. https://doi.org/10.1515/revce-2015-0021

[31] Suhaimi, H., Wang, S., Thornton, T., & Das, D. B. (2015). On glucose diffusivity of tissue engineering membranes and scaffolds. *Chemical Engineering Science, 126*, 244–256. https://doi.org/10.1016/j.ces.2014.12.029

[32] Mekala, S., Silva, E. K., & Saldaña, M. D. A. (2022). Ultrasound-assisted production of emulsion-filled pectin hydrogels to encapsulate vitamin complex: Impact of the addition of xylooligosaccharides, ascorbic acid and supercritical CO2 drying. *Innovative Food Science & Emerging Technologies, 76*, 102907. https://doi.org/10.1016/j.ifset.2021.102907

[33] Wathoni, N., *et al.* (2019). Characterization and antioxidant activity of pectin from Indonesian mangosteen (*Garcinia mangostana* L.) rind. *Heliyon, 5*, e02299. https://doi.org/10.1016/j.heliyon.2019.e02299

[34] Mishra, R. K., Datt, M., Pal, K., & Banthia, A. K. (2008). Preparation and characterization of amidated pectin based hydrogels for drug delivery system. *Journal of Materials Science: Materials in Medicine, 19*(6), 2275–2280. https://doi.org/10.1007/s10856-007-3310-4

[35] Nguyen, H. T. L., Katopo, L., Pang, E., Mantri, N., & Kasapis, S. (2019). Structural variation in gelatin networks from low to high-solid systems effected by honey addition. *Food Research International, 121*, 319–325. https://doi.org/10.1016/j.foodres.2019.03.048

[36] Synytsya, A., Čopíková, J., Matějka, P., & Machovič, V. (2003). Fourier transform Raman and infrared spectroscopy of pectins. *Carbohydrate Polymers, 54*(1), 97–106. https://doi.org/10.1016/S0144-8617(03)00158-9

[37] Liu, Z., *et al.* (2024). Investigating the effect of pH on the swelling process, mechanical and thermal attributes of polyacrylamide hydrogel structure: A molecular dynamics study. *Case Studies in Thermal Engineering, 55*, 104148. https://doi.org/10.1016/j.csite.2024.104148

[38] Liu, G., *et al.* (2023). Synthesis of a polyacrylamide hydrogel modified with a reactive carbamate surfactant: Characterization, swelling behavior, and mathematical models. *Colloids and Surfaces A: Physicochemical and Engineering Aspects, 677*, 132403. https://doi.org/10.1016/j.colsurfa.2023.132403

[39] Razavi, R., & Kenari, R. E. (2023). Ultraviolet–visible spectroscopy combined with machine learning as a rapid detection method to the predict adulteration of honey. *Heliyon, 9*(10), e20973. https://doi.org/10.1016/j.heliyon.2023.e20973

[40] Ma, X., *et al.* (2014). A novel chitosan–collagen-based hydrogel for use as a dermal filler: Initial in vitro and in vivo investigations. *Journal of Materials Chemistry B, 2*(18), 2749–2763. https://doi.org/10.1039/C3TB21842B

[41] Valipour, F., Rahimabadi, E. Z., & Rostamzad, H. (2023). Preparation and characterization of wound healing hydrogel based on fish skin collagen and chitosan cross-linked by dialdehyde starch. *International Journal of Biological Macromolecules, 253*, 126704. https://doi.org/10.1016/j.ijbiomac.2023.126704

Appendix A

Table A1 provides a comprehensive quantitative analysis of the swelling behavior of hydrogel samples, showcasing the average, minimum, and maximum weights measured at designated time intervals. This table methodically differentiates between air-dried and vacuum-dried samples, ensuring clarity in the presentation of data. Such detailed tabulation is crucial for assessing the consistency and variability of the hydrogels' swelling responses across different experimental setups. It serves as a key resource for evaluating the hydrogels' performance under varied conditions, highlighting the impact of drying methods on their physical properties and efficacy.

Table A1. Weights of the hydrogel at different times during the swelling test, for the different samples

Time (min)	Sample 1	Sample 2		Sample 3		Sample 4		Sample 5	
	Air Dry	Air Dry	Vac Dry	Air Dry	Vac Dry	Air Dry	Vac Dry	Air Dry	Vac Dry
0	0.649 (0.629-0.657)	1.032 (0.967-1.150)	0.833 (0.544-0.994)	1.676 (1.655-1.692)	1.865 (1.648-2.062)	1.616 (1.444-1.902)	1.479 (1.245-1.604)	2.223 (1.960-2.614)	1.823 (1.686-1.896)
5	0.951 (0.925-0.971)	1.294 (1.279-1.314)	1.132 (0.802-1.359)	1.877 (1.853-1.896)	2.112 (1.878-2.341)	1.810 (1.598-2.157)	1.625 (1.342-1.849)	2.363 (2.061-2.834)	1.981 (1.838-2.066)
10	1.086 (1.062-1.119)	1.505 (1.413-1.557)	1.247 (0.973-1.424)	2.032 (2.009-2.052)	2.205 (1.913-2.547)	1.904 (1.598-2.267)	1.738 (1.401-2.033)	2.407 (2.096-2.899)	2.032 (1.849-2.192)
15	1.309 (1.215-1.363)	1.611 (1.526-1.661)	1.446 (1.153-1.620)	2.051 (2.026-2.072)	2.235 (1.890-2.602)	1.929 (1.699-2.269)	1.756 (1.435-2.021)	2.405 (2.127-2.833)	2.043 (1.861-2.199)
20	1.454 (1.442-1.467)	1.704 (1.584-1.772)	1.656 (1.610-1.702)	2.121 (2.097-2.140)	2.305 (1.948-2.695)	1.978 (1.681-2.375)	1.767 (1.376-2.067)	2.342 (2.106-2.774)	2.076 (1.938-2.148)
25	1.576 (1.547-1.596)	1.729 (1.630-1.787)	1.716 (1.688-1.743)	2.151 (2.140-2.160)	2.398 (2.086-2.698)	1.996 (1.773-2.380)	1.789 (1.366-2.107)	2.254 (1.989-2.742)	2.026 (1.876-2.105)
30	1.620 (1.602-1.634)	1.772 (1.649-1.842)	1.755 (1.734-1.776)	2.149 (2.139-2.155)	2.418 (2.112-2.709)	2.048 (1.812-2.283)	-	-	-

*Weights are given as average (min-max)